Accepted Manuscript

Antifungal activity, mode of action variability, and subcellular distribution of coumarin-based antifungal azoles

Rebecca Elias, Raphael I. Benhamou, Qais Z. Jaber, Orly Dorot, Sivan Louzoun Zada, Keren Oved, Edward Pichinuk, Micha Fridman

PII: S0223-5234(19)30624-5

DOI: https://doi.org/10.1016/j.ejmech.2019.07.003

Reference: EJMECH 11500

To appear in: *European Journal of Medicinal Chemistry*

Received Date: 14 May 2019

Revised Date: 30 June 2019

Accepted Date: 1 July 2019

Please cite this article as: R. Elias, R.I. Benhamou, Q.Z. Jaber, O. Dorot, S.L. Zada, K. Oved, E. Pichinuk, M. Fridman, Antifungal activity, mode of action variability, and subcellular distribution of coumarin-based antifungal azoles, *European Journal of Medicinal Chemistry* (2019), doi: https://doi.org/10.1016/j.ejmech.2019.07.003.

Antifungal Activity, Mode of Action Variability, and Subcellular Distribution of Coumarin-based Antifungal Azoles

Rebecca Elias,[a] *Raphael I. Benhamou,*[a] *Qais Z. Jaber,*[a] *Orly Dorot,*[b] *Sivan Louzoun Zada*[a] *Keren Oved,*[b] *Edward Pichinuk,*[b] *and Micha Fridman*[a]*.

[a] School of Chemistry, Raymond & Beverly Sackler Faculty of Exact Sciences, Tel Aviv University, Tel Aviv, 6997801, Israel. [b] Blavatnik Center for Drug Discovery, Tel Aviv University, Tel Aviv, 6997801, Israel.

*Correspondence to: mfridman@tauex.tau.ac.il

KEY WORDS: Antifungals; Fluorescent Imaging, Antifungal Azoles, Organelle targeting

ABBREVIATIONS

CYP: Cytochrome P450; CYP3A4: Cytochrome P450 3A4; CYP51: cytochrome P450 lanosterol 14α-demethylase; ER: endoplasmic reticulum; IC_{50}: concentration toxic to 50% of the enzyme; MIC: minimal inhibitory concentration; MTT: 3-(4,5- dimethylthiazol-2-yl)-2,5-diphenyltetrazolium bromide; SAR: activity relationship study; ZOI: zone of inhibition.

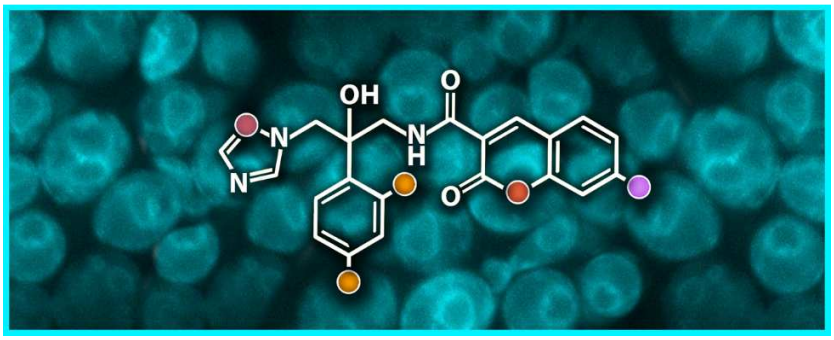

ABSTRACT

Azole antifungals inhibit the biosynthesis of ergosterol, the fungal equivalent of cholesterol in mammalian cells. Here we report an investigation of the activity of coumarin-substituted azole antifungals. Screening against a panel of *Candida* pathogens, including a mutant lacking CYP51, the target of antifungal azoles, revealed that this enzyme is inhibited by triazole-based antifungals, whereas imidazole-based derivatives have more than one mode of action. The imidazole-bearing antifungals more effectively reduced trailing growth associated with persistence and/or recurrence of fungal infections than triazole-based derivatives. The imidazole derivatives were more toxic to mammalian cells and more potently inhibited the activity of CYP3A4, which is one of the main causes of azole toxicity. Using live cell imaging, we showed that regardless of the type of azole ring fluorescent 7-diethylaminocoumarin-based azoles localized to the endoplasmic reticulum, the organelle that harbors CYP51. This study suggests that the coumarin is a promising scaffold for development of novel azole-based antifungals that effectively localize to the fungal cell endoplasmic reticulum.

INTRODUCTION

The incidence of severe fungal infections has risen sharply in recent decades, due in large part to a considerable increase in the number of immunosuppressed and/or immunocompromised patients.[1,2] Moreover, fungal infections are increasingly being caused by drug-resistant strains with members of *Candida* genus, in particular *Candida albicans* and *Candida glabrata*, the most frequently encountered fungal pathogens.[3–7] Thus, antifungal drug development is a high priority.

Alarmingly, prevention and treatment of fungal infections relies on a very limited number of drugs belonging to three main classes: the azoles, the polyenes, and 5-fluorocytosine.[8–10] The azole antifungals are commonly used as first line treatment of both topical and invasive fungal infections worldwide.[11,12] Members of the azole class inhibit lanosterol 14α-demethylase (CYP51), a cytochrome P450 that catalyzes a demethylation step in the biosynthesis of the fungal plasma-membrane sterol ergosterol.[13–15] Notably, an orthologue of the fungal CYP51 is found in mammals, and humans express many cytochrome P450 enzymes.[14] First-generation azole drugs such as ketoconazole (**1**), miconazole (**2**), and clotrimazole (**3**) can cause hepatotoxic effects, impairment of gastrointestinal and endocrine functions, and skin irritation. The second-generation azoles (*i.e.*, itraconazole (**4**) and fluconazole (**5**)) and third-generation drugs (*i.e.*, voriconazole (**6**) and posaconazole (**7**)) display markedly improved safety profiles and better oral bioavailability.[16] Unfortunately, however, all three generations of azole antifungals inhibit mammalian cytochrome P450s.[17,18] Global increase in cases of resistance to antifungal azoles and side effects associated with the systemic use of azole antifungals have driven the exploration for new types of antifungal azoles in recent years.[19–24]

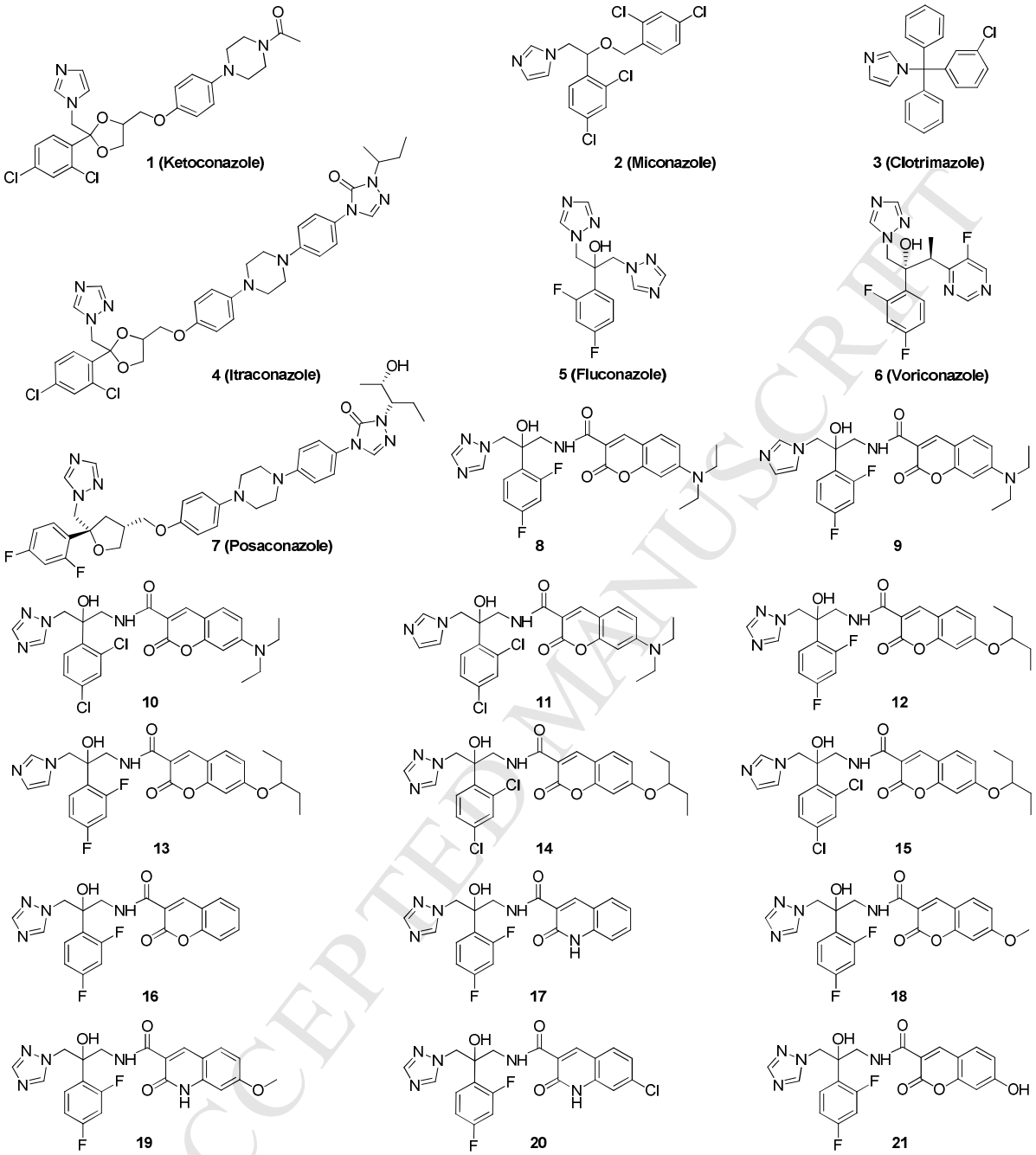

Figure 1. Structures of clinically used antifungal azoles **1-7**, which were used as controls in this study, and of coumarin- and quinolone-based antifungal azole derivatives **8**–**21**.

In designing novel antifungal azoles, perturbations in the activities of heme proteins, especially P450 isoforms present in mammalian cells, must be reduced or, ideally, avoided. In

humans, CYP3A4 makes up the largest fraction of the total CYP content in the liver and intestines; this enzyme is responsible for the metabolism of multiple small molecules. CYP3A4 is unique from other major CYPs in its exceptionally relaxed substrate selectivity. As a result, it is estimated that this enzyme is responsible for metabolizing over 50% of the marketed drugs. As a result, CYP3A4 inhibition is one of the main causes of adverse drug/drug and drug/food interactions. Unfortunately, all clinically used antifungal azoles inhibit CYP3A4. Second- and third-generation azole antifungals vary in CYP3A4 inhibition potency: **4** and **7** are more potent inhibitors than are **5** and **6**.[25–27]

CYP51 and a number of other enzymes involved in the biosynthesis of ergosterol localize primarily to the endoplasmic reticulum (ER).[9,28] By designing inherently fluorescent antifungal azole derivatives we recently discovered that certain azole antifungals localize mainly to the mitochondria.[29] We therefore reasoned that these antifungal azoles do not reach their target in the ER. Based on this hypothesis, we developed antifungal azole **8** by attaching a 7-(diethyl)-aminocoumarin fluorescent segment to the pharmacophore of the antifungal azole fluconazole (**5**) (Figure 1).[30] Azole **8** localizes primarily to the ER in *Candida* cells, and its antifungal activity was 4- to 64-fold more potent than that of fluconazole against a panel of *Candida* strains.

To explore the potential of coumarin-based azole antifungals we conducted a structure activity relationship (SAR) investigation of a collection of coumarin-based and 2-quinolone-based azoles that were systematically altered at four structural motifs. These compounds were evaluated with respect to antifungal activity, mode of action, subcellular localization, target selectivity, and toxicity to mammalian cells.

RESULTS AND DISCUSSION

Synthesis of coumarin- and quinolone-based azole antifungals

To study the SAR of ER-localizing antifungal azole **8**, we generated derivatives **9–21** by altering one or more of four different chemical functionalities of this azole scaffold: the two halogen atom substituents on the phenyl ring, the azole ring, the hetero-atom (oxygen in the coumarin scaffold or an NH in the 2-quinolone scaffold), and the substituent at the C7 position of the coumarin or 2-quinolone (R_1-R_4, respectively, Scheme 1). Several of the marketed azole antifungals including **1**, **2**, and **4** (Figure 1) are racemic mixtures. Computer simulated docking of the *R* and *S* enantiomers of aminocoumarin-based azole **8** revealed that the interactions with cytochrome P450DM take place through a similar binding mode;[29] therefore, the azole antifungals in this study were synthesized and evaluated as racemic mixtures.

Briefly, nucleophilic displacement of the chloride atom of commercially available α-chloro-2,4-di-halo-acetophenones **1a** and **1b** by an imidazole or a triazole ring gave the corresponding azole intermediate compounds **2a-d** (Scheme 1). Conversion of the ketones of **2a-d** to the corresponding racemic mixtures of epoxides using trimethylsulfoxonium iodide in the presence of a base gave intermediates **3a-d**, which were then reacted with sodium azide to afford intermediates **4a-d**. Catalytic hydrogenation of **4a-d** gave free amine intermediates **5a-d**, which were coupled to the free carboxylic acid functionality of the coumarins and 2-quinolones to yield antifungal azoles **8-21** (Figure 1). Antifungal azoles **9-21** were characterized by ^{1}H and ^{13}C NMR as well as by ^{19}F NMR when applicable and by HRMS**;** purities were ≥95% as determined by HPLC (see Experimental section and Supplementary Material for NMR spectra and HPLC traces).

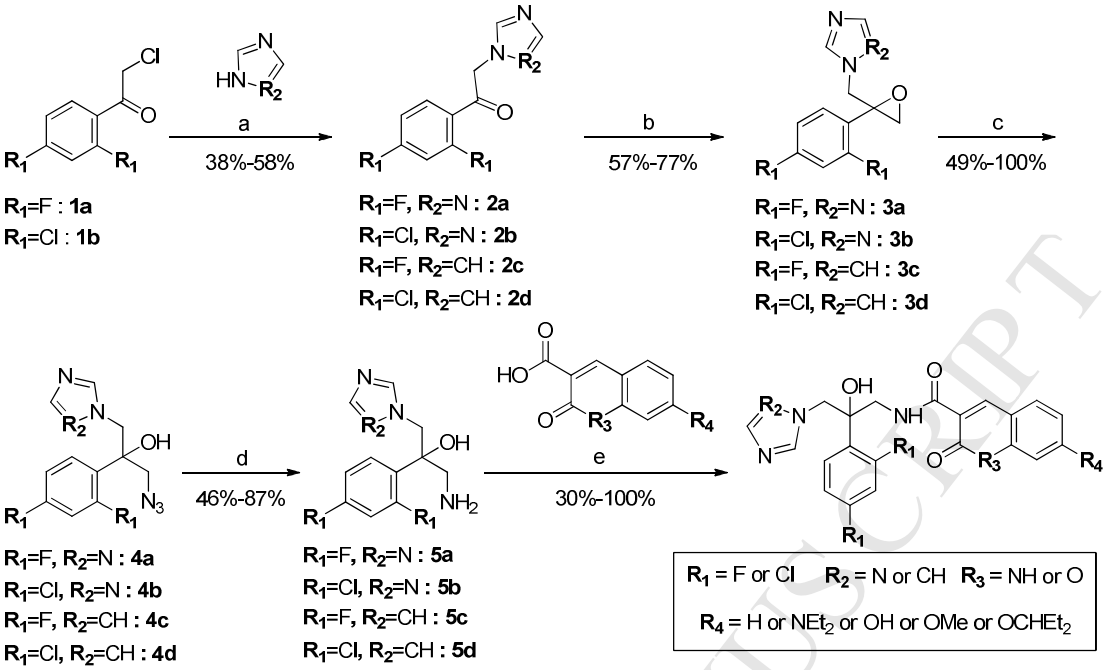

Scheme 1. Synthesis of coumarin- and 2-quinolone-based antifungal azoles. Reagents and conditions: a) $NaHCO_3$, toluene, reflux, 4 h; b) trimethylsulfoxonium iodide, 20% NaOH, toluene, 60 °C, 4 h; c) NaN_3, DMF, 65 °C, 12 h; d) H_2, palladium on carbon, isopropanol, room temperature overnight; e) HATU, DIPEA, DMF, room temperature overnight.

Coumarin-based azoles display potent anti-*Candida* activity

To test antifungal activity we chose 10 strains representing different species of *Candida*, the most common human fungal pathogenic genus, which cause both superficial and systemic infections (Table 1).[31] The chosen panel included *C. albicans* (Strains A-C), *C. glabrata* (Strains D-F), *C. parapsilosis* (Strains G, H), *C. guilliermondii* (Strain I) and *C. dubliniensis* (Strain J). To evaluate antifungal activity we determined the minimal inhibitory concentration (MIC) values for each of the azoles using the broth microdilution method over a concentration range of 0.007–64 μg/mL. The antifungal activities of azoles **8-21** and of seven clinically used azoles including first-generation (**1**, **2**, and **3**), second-generation (**4** and **5**), and third-generation (**6** and **7**) were evaluated (Table 1).

Table 1. Minimal inhibitory concentration (MIC) values [µg/mL].

	Yeast Strains [a]									
Comp. #	**A**	**B**	**C**	**D**	**E**	**F**	**G**	**H**	**I**	**J**
1	0.007	0.007	0.007	1	1	0.06	0.007	0.007	0.007	0.007
2	0.007	0.007	0.007	2	1	0.06	0.06	0.003	0.06	0.06
3	0.007	0.007	0.007	4	0.5	0.06	0.007	0.007	0.007	0.007
4	0.007	0.007	0.007	1	1	0.125	0.007	0.03	0.03	0.06
5	0.5	0.25	0.25	64	64	8	1	2	4	4
6	0.007	0.007	0.007	0.5	2	0.125	0.015	0.03	0.06	0.06
7	0.007	0.007	0.007	1	1	0.125	0.015	0.03	0.03	0.03
8	0.06	0.06	0.03	4	16	8	0.125	1	1	1
9	0.015	0.06	0.06	8	8	2	0.015	0.125	0.5	0.5
10	0.03	0.03	0.03	4	16	4	0.06	0.5	0.25	0.5
11	0.015	0.03	0.03	4	2	0.25	0.015	0.06	0.125	0.25
12	0.125	0.125	0.25	>64	32	4	0.5	2	2	2
13	0.03	0.015	0.03	2	4	1	0.125	0.25	0.125	0.25
14	0.06	0.03	0.06	>64	>64	2	0.25	0.5	0.5	0.5
15	0.03	0.06	0.06	2	2	0.5	0.125	0.5	0.25	0.25
16	0.25	0.125	0.25	1	4	1	0.25	2	1	0.5
17	2	1	0.5	>64	64	16	2	8	8	8
18	0.25	0.125	0.5	32	8	4	0.25	2	1	4
19	1	2	4	>64	>64	>64	2	>64	>64	>64
20	1	1	0.5	64	>64	16	1	8	8	8
21	64	64	>64	>64	64	>64	>64	>64	>64	>64

[a] **A** = *C. albicans* 90028; **B** = *C. albicans* P-87; **C** = *C. albicans* SN152; **D** = *C. glabrata* 66032; **E** = *C. glabrata* 2001; **F** = *C. glabrata* 192; **G** = *C. parapsilosis* 90018; **H** = *C. parapsilosis* 22019; **I** = *C. guilliermondii* T-47; **J** = *C. dubliniensis* T-99. MIC values were determined using the broth double-dilution method starting from a concentration of 64 µg/mL. Cells were grown in Casitone medium at 37 °C under CO_2 for 24 h. Each concentration was tested in triplicate, and results were confirmed in two independent sets of experiments.

Displacement of the 1,2,4-triazole ring with an imidazole enhanced antifungal activity. Compared to the 1,2,4-triazole-based antifungal azoles **8**, **10**, **12**, and **14**, the MIC values of the corresponding imidazole-based compounds **9**, **11**, **13**, and **15**, respectively, were 2- to 32-fold lower against the majority of the tested strains and were equally potent against the rest. The coumarin-based azoles **8-11**, which contain a 7-diethylaminocoumarin, displayed the most potent and broad spectrum antifungal activity.

Comparison between the MIC values of azole **12** and azole **18**, differing solely by the C7 substituent (R_4, Scheme 1) of the coumarin segment, revealed that the alkyl group on the ether did not significantly impact either spectrum of activity or potency. Interestingly, the 7-hydroxy coumarin-based azole **21** did not inhibit the growth of any strain in the panel (MIC $\geq$ 64 µg/mL, Table 1). Although certain differences in the structure of the alkyl ether at the C7-position of the coumarin are tolerated, the presence of an alcohol at this position completely abrogates antifungal activity. This may be explained by the incompatibility of the hydrophilic alcohol in the highly hydrophobic pocket at the catalytic domain of CYP51.[32,33] Of the 14 coumarin- and 2-quinolone-based azoles, 7-diethylaminocoumarin-based azoles **10** and **11** and 7-(1-ethylpropoxy)-coumarin based azoles **13** and **15** displayed the best activity against the non-albicans *Candida* strains tested.

Finally, similar to the third-generation azoles **6** and **7**, 7-diethylaminocoumarin-based azoles **8-11** and 7-(1-ethylpropoxy)-coumarin-based azoles **12-15** displayed potent activity against the tested *C. albicans* strains with MIC values of 0.007-0.125 µg/mL. These derivatives had better antifungal activity than the second-generation antifungal azole **5**, which, due to low cost, is most commonly used for treatment of fungal infections worldwide.

Imidazole-based derivatives inhibit CYP51 as well as other critical fungal processes

It was previously reported that, in addition to inhibition of CYP51-mediated ergosterol biosynthesis, clinically used azole antifungals such as **1** and **2** (Figure 1) inhibit the activity of a variety of additional targets including the activities of several membrane-bound enzymes.[8] To identify the structural motifs associated with selective inhibition of CYP51 and those that contribute to other antifungal effects, we compared the antifungal activities of representative coumarin-based azoles in a mutant strain lacking copies of both the *ERG11* and *ERG3* genes. *ERG11* encodes CYP51, the target of antifungal azoles, which is essential for fungal cell growth under aerobic conditions when the C-5 sterol desaturase-encoding *ERG3* is expressed.[34,35] The *erg11*ΔΔ *erg3*ΔΔ mutant strain is therefore viable despite the absence of CYP51.

The effects of 1,2,4-triazole-based azoles **8** and **10** and imidazole-based azoles **9** and **13** and control drugs were analyzed using the disk diffusion assay against the double knockout strain and the parental strain SN152 (Figure 2). A zone of growth inhibition was visible after 24 hours in plates seeded with the parental strain and treated with disks containing 1,2,4-triazole-based azoles **5**, **6**, **8**, or **10**; these compounds did not inhibit growth of the *erg11*ΔΔ *erg3*ΔΔ mutant, however (Figure 2). These results indicate that CYP51 is the main target of the 1,2,4-triazole-based azole antifungals tested. The imidazole-based azoles (**1**, **2**, **9**, and **13**) inhibited growth of both the parental strain and of the mutant (Figure 2). Thus, the imidazole-based azoles affect more than one process in the fungal cells.

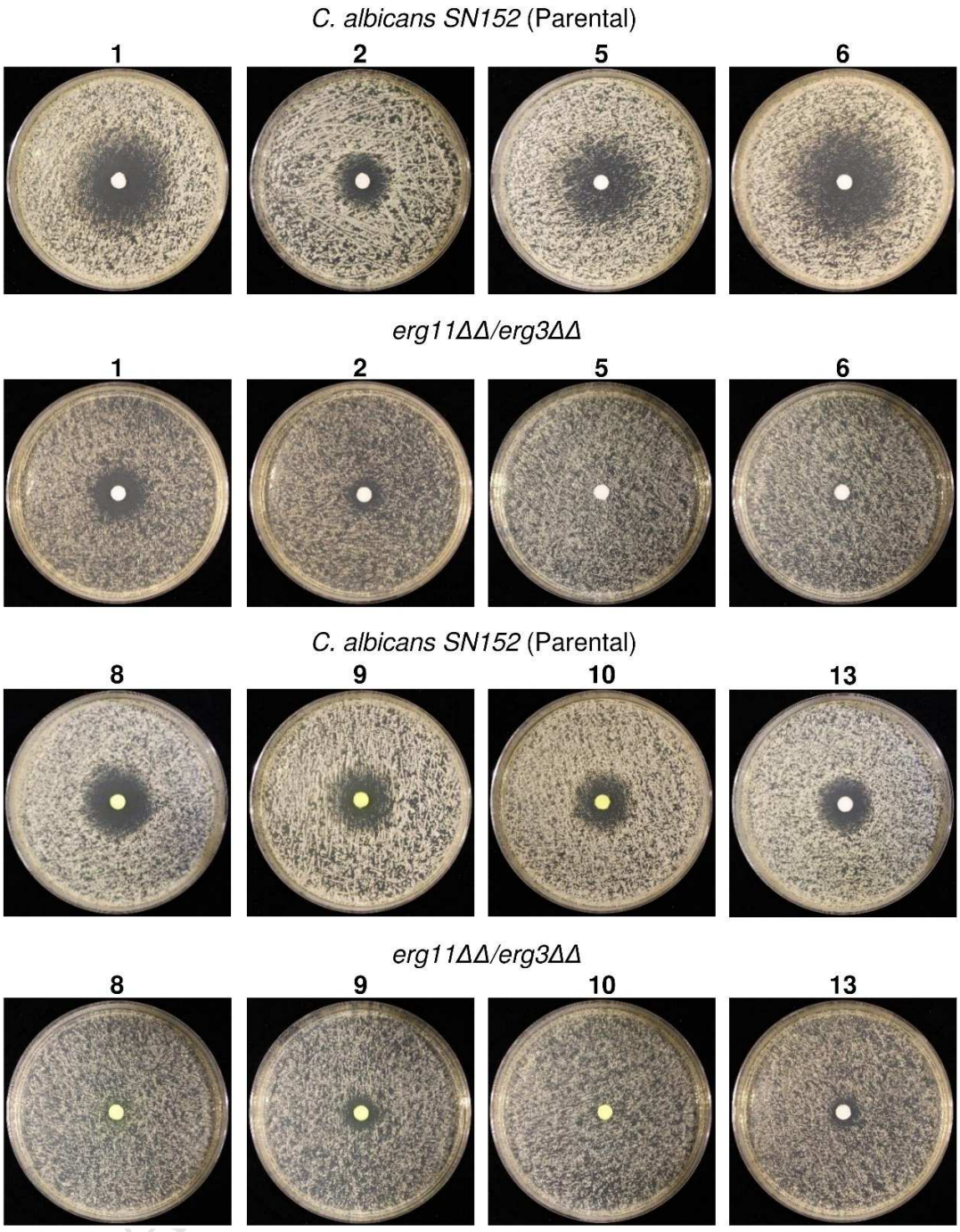

Figure 2. Activity of azole antifungals against CYP51-deficient yeast. *C. albicans* strains SN152 (parental) and the *erg11*ΔΔ *erg3*ΔΔ mutant were plated onto casitone plates and allowed to grow in the presence of a disk containing 25 µg of the indicated compound at 30 °C for 24 h. Photographs of representative plates are shown.

Imidazole-based compounds reduce drug tolerance

Fungal susceptibility is commonly determined quantitatively *in vitro* by analysis of MIC values after 24 h of growth in the presence of the tested antimicrobial agent. However, MIC measurements do not measure residual growth, also termed tolerance or trailing.[36,37] Tolerance occurs when subpopulations of fungal cells multiply despite prolonged exposure to an antifungal drug, and this property can contribute to the persistence and/or recurrence of fungal infections. An increase in MIC value after exposure to a drug is indicative of tolerance. To evaluate the level of tolerance, we compared MIC values after 24 hours of incubation to those measured after 48 hours against two *C. albicans* and two *C. glabrata* strains (Table 2).

Table 2. MIC values [µg/mL] at 24 and 48 hours.[a]

Compound	**Yeast strain**							
	***C. albicans* 90028**		***C. albicans* SN152**		***C. glabrata* 66032**		***C. glabrata* 192**	
	24 hours	**48 hours**	**24 hours**	**48 hours**	**24 hours**	**48 hours**	**24 hours**	**48 hours**
1	0.007	0.007	0.007	0.007	1	4	0.06	0.125
2	0.007	0.015	0.007	0.015	2	4	0.06	0.125
3	0.007	0.007	0.007	0.007	4	4	0.06	0.25
4	0.007	0.007	0.007	0.007	1	>64	0.125	0.125
5	0.5	0.5	0.25	1	64	>64	8	8
6	0.007	0.007	0.007	0.007	0.5	4	0.125	0.25
7	0.007	0.007	0.007	0.007	1	>64	0.125	0.125
8	0.06	0.125	0.03	0.125	4	>64	8	>64
9	0.015	0.06	0.06	0.125	8	32	2	4
10	0.03	0.06	0.03	0.06	4	>64	4	>64
11	0.015	0.03	0.03	0.06	4	>64	0.25	1
12	0.125	0.5	0.25	0.5	>64	>64	4	8
13	0.03	0.06	0.03	0.06	2	4	1	2
14	0.06	0.06	0.06	0.06	>64	>64	2	>64
15	0.03	0.06	0.06	0.06	2	>64	0.5	1

[a] MIC values were determined using the broth double-dilution method staring from a concentration of 64 µg/mL. Cells were grown in Casitone medium at 37 °C under CO_2. Each concentration was tested in triplicate, and results were confirmed in two independent sets of experiments.

Tolerance was more significant for the *C. glabrata* strains than for the *C. albicans* strains. We observed higher MIC values for all tested azoles for *C. glabrata* ATCC 66032 at 48 hours than at 24 hours (Table 2). Interestingly, of the clinically used azoles, the imidazole-based drugs **1**, **2**, and **3** maintained better efficacy over time with 48-hour MIC values no more than two double dilutions higher than 24-hour MIC values against *C. glabrata* ATCC 66032 (Table 2). In contrast, significant trailing growth of *C. glabrata* ATCC 66032 was observed for the triazole-based compounds **4**, **5**, **6**, and **7** (Table 2). For example, the 48-hour MIC of **7** was 64-fold higher than the 24-hour MIC value against this strain.

The coumarin-based azoles **8-15** are pairs of compounds that vary solely in the azole ring. Although MIC values measured after 48 hours were generally higher than those at 24 hours, there was less tolerance in samples treated with imidazoles **9**, **11**, **13**, and **15** than in samples treated with triazoles **8**, **10**, **12**, and **14**. Since we showed that the antifungal activity of the imidazoles is not based solely on the inhibition of CYP51, the reduction in trailing growth likely results from the non-CYP51-targeted activity of the imidazole-based compounds.

Imidazole ring leads to more potent inhibition of human CYP3A4

Inhibition of human CYP3A4 is an undesired activity that is associated with the toxicity of antifungal azoles.[18] The ability of the coumarin-based azoles to inhibit CYP3A4 was determined in an assay with recombinant human CYP3A4.[38] The results are summarized in Table 3. Of the clinically used azoles tested, imidazoles **1** and **3** potently inhibited CYP3A4 with **3** displaying the most potent enzymatic inhibition among all antifungals tested in this study (Table 3). Of the clinically used triazoles tested, **5** was the poorest CYP3A4 inhibitor, whereas the third-generation azole **7** potently inhibited the enzyme. Similar to the effects of the imidazole

ring on antifungal activity, comparison between the inhibition of CYP3A4 by the triazole derivatives of coumarin-based azoles **8**, **10**, **12** and **14** and their corresponding imidazole-based compounds **9**, **11**, **13** and **15** revealed that the imidazole ring leads to more potent inhibition of this CYP. An exception was observed for aminocoumarin-based triazole **8** and its imidazole derivative **9**, which had similar IC_{50} values (~1 µM, Table 3).

Table 3. CYP3A4 inhibition by azole derivatives.[a]

Compound	IC_{50} [µM]
1	0.1826 ± 0.0337
3	0.0670 ± 0.0089
5	23.9698 ± 4.8783
6	≥ 2.5[b]
7	0.6721 ± 0.1696
8	1.0223 ± 0.1403
9	1.3123 ± 0.2440
10	0.3512 ± 0.0426
11	0.1272 ± 0.0104
12	≥ 2.5[b]
13	0.3320 ± 0.0482
14	≥ 2.5[b]
15	0.2515 ± 0.0558

[a] Inhibition of CYP3A4 was quantified in an assay with recombinant CYP3A4. Experiments were performed in duplicate at 37 °C. [b] The highest tested concentration due to solubility limitations under the assay conditions.

These results suggest that, in general, imidazole-based antifungal azoles are more effective inhibitors of CYP3A4 and are, therefore, less CYP51-selective than the corresponding triazole-based antifungal azoles. These results also suggest that the residual antifungal activity of the

coumarin-based azoles bearing an imidazole-ring in the strain lacking CYP51 may stem from non-selective inhibition of other heme-containing monooxygenases in fungal cells.

Imidazole ring is associated with toxicity to mammalian cells

We next quantified the effects of the antifungal azoles on the viability mammalian HepG2 cells, an immortalized human liver hepatocellular carcinoma cell line, and HEK-293T cells, an immortalized human embryonic kidney cell line. We studied coumarin-based azoles **10** and **14**, which bear 1,2,4-triazole rings, and the corresponding imidazole analogues **11** and **15**, respectively, as well as **1**, **5**, **6**, and **7**. The cells were treated with each of the azoles at concentrations ranging from 5 to 50 μM for 24 h, after which cell viability was evaluated using the 3-(4,5- dimethylthiazol-2-yl)-2,5-diphenyltetrazolium bromide (MTT) assay. The maximal tested concentration of 50 μM was determined based on solubility limitations of some of the coumarin-based azoles and control drugs. Notably, at the maximal concentration tested, none of azole antifungals reduced viability of the mammalian cells tested by more than 40% (Figure 3).

Of the clinically used azoles, **1** and **7** were the most toxic, and **5** had the smallest effect on cell viability (Figure 3). The clinically used azoles **5**, **6**, and **7** share the same pharmacophore composed of a 1,2,4-triazole and difluorophenyl ring. The additional segments attached to the pharmacophore in these clinically used antifungals are distinctly different (Figure 1). The fact that **7** was more toxic to the tested mammalian cells than was **5** indicates that although the imidazole ring has a major effect on mammalian cell toxicity the moieties attached to the pharmacophore moderate cell toxicity. Of coumarin-based azoles tested, 7-diethylaminocoumarin-based imidazole **11** was the most toxic to both tested cells lines, and the corresponding triazole **10** was the least toxic; the differences in the toxicity of the 7-(1-ethylpropoxy)-coumarin-based azoles **14** and **15** were less pronounced (Figure 3).

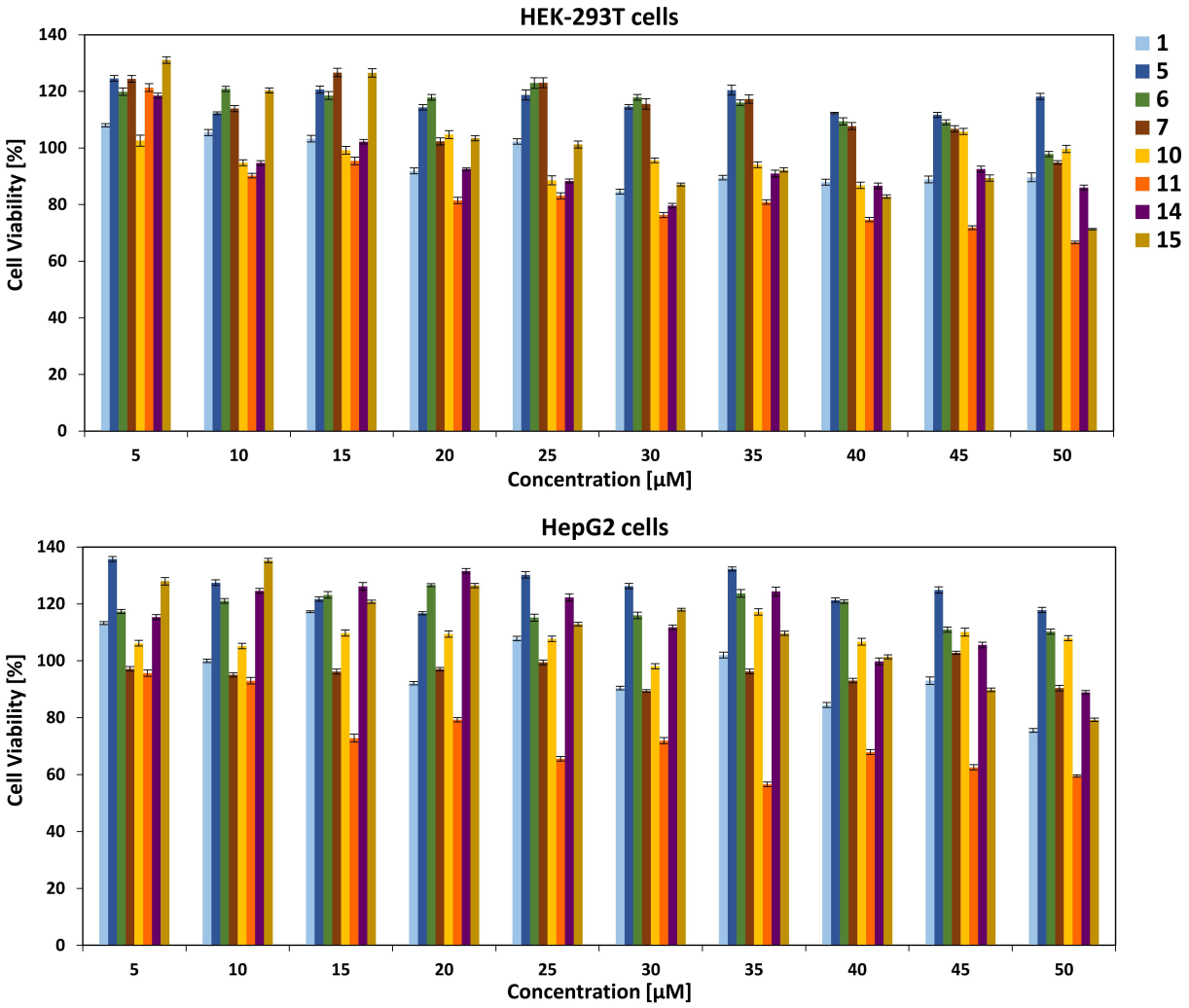

Figure 3. Viability of HEK-293T and HepG2 cells in the presence of azole antifungals. Cells were allowed to grow in the presence of indicated concentration of azole derivative for 24 h at 37 °C. Viability is plotted as percent of vehicle-treated control cells. Experiments were performed in triplicate, and the results were obtained from two independent experiments.

Subcellular distribution in live *Candida* cells is not affected by the type of azole ring

We previously demonstrated the use of inherently fluorescent antifungal azoles for determination of the subcellular distribution of the molecule in live *Candida* cells during the first few hours after exposure to the azole.[29,30,39] Notably, the subcellular distributions of the free

fluorescent dyes differed from those of the corresponding fluorescent azole antifungals suggesting that the staining pattern is not determined by the dye segment alone.

Since there are distinctive differences in biological activities of antifungal azoles depending on the type of the azole ring, we asked if the azole ring affects subcellular distribution by analyzing the subcellular localization of azoles **8** and **9**, which differ in their azole ring (1,2,4-triazole and imidazole, respectively) contain the 7-diethylaminocoumarin fluorophore that proved suitable for live cell imaging experiments in *Candida* yeast cells. Subcellular localization was evaluated in *Candida albicans* SN152 and in *Candida glabrata* 2001 yeast cells. A distinct and typical circular ER structure around the nuclear envelope with peripheral cortical extensions [39] was clearly visible in both *C. glabrata* and *C. albicans* yeast cells stained with the azoles (Figure 4). Previously, we showed that azole antifungals with different fluorophores including dansyl and cyanine 5 can localize to different organelles.[29] However, staining patterns were similar for azoles **8** and **9**. Although the activities of these two azoles varied significantly in most of the assays in this study, the results of the fluorescent imaging experiments clearly indicated that the type of azole ring did not affect the subcellular distribution.

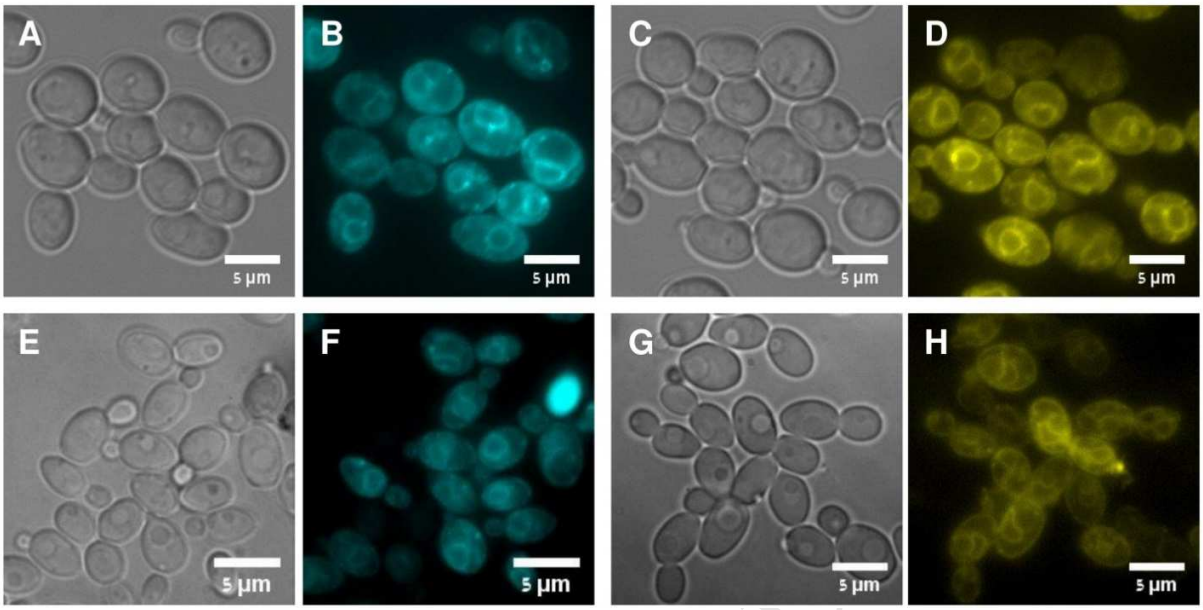

Figure 4. Fluorescent imaging of azoles 8 and 9 in live *Candida* cells. A-B) *C. albicans* SN152 cells incubated for 60 min with azole **8** (cyan, 10 µM), C-D) *C. albicans* SN152 cells incubated for 60 min with azole **9** (yellow, 10 µM), E-F) *C. glabrata* 2001 cells incubated for 60 min with azole **8** (cyan, 10 µM), and G-H) *C. glabrata* 2001 cells incubated for 60 min with azole **9** (yellow, 10 µM). For each azole and yeast cell strain, the bright field image is shown on the left and the fluorescent image is on the right. The bandpass filters used to image the fluorescent azoles were ex: 427 nm and em: 510 nm. Scale bars, 5 µm.

CONCLUSIONS

A series of 11 coumarin-based and three 2-quinolone-based azoles were synthesized by systematically altering four structural motifs. From analyses of biological activities of these compounds, we were able to generate high-resolution structure activity relationship insights. The imidazole-containing antifungal azoles had higher efficacy against a diverse panel of *Candida* pathogens than their corresponding 1,2,4-triazole analogues. Unlike the MIC values of the

triazoles, the MIC values of the imidazole-bearing compounds were more similar at 24 and 48 hours, indicating that the yeast strains are less tolerant to the imidazole-based azoles. Since drug tolerance is associated with persistence and reoccurrence of infection, this feature is of particular importance. The antifungal activity of the triazole-based azoles was dependent on expression of CYP51, the target of the azole antifungals. In contrast, imidazole-based compounds displayed antifungal activity against a mutant lacking CYP51 indicating that imidazole-based azole antifungals have additional modes of action. The imidazole-based compounds were more toxic to mammalian cells and more potently inhibited CYP3A4 than the triazole-based antifungals. CYP3A4 is one of the most abundant human cytochrome P450s, a family of enzymes that are important for the metabolism of endogenous and exogenous compounds.

By taking advantage of the suitability of the 7-diethylaminocoumarin fluorescence for live-cell imaging, we showed that although the type of the azole ring affects the antifungal activity, selectivity, and mode of action, it does not influence the subcellular distribution of the azole compounds in yeast cells. The two derivatives evaluated were identical except that one had a triazole and the other an imidazole ring; both localized to the ER. This is of particular importance since we recently reported that by targeting the drug to the ER, which harbors CYP51, the antifungal activity of an azole antifungal can be enhanced. To conclude, this study suggests that coumarin residues are promising scaffolds for development of novel azole-based antifungals that effectively localize to the endoplasmic reticulum.

EXPERIMENTAL SECTION

Chemistry

General methods and instrumentation: ^{1}H-NMR spectra were recorded on BrukerAvance™ 400 or 500 MHz spectrometers, and chemical shifts (reported in ppm) were calibrated to $CDCl_3$ (d = 7.26) when $CDCl_3$ was the solvent, to CD_3OD (d = 3.31) when CD_3OD was the solvent and to DMSO (d = 2.50) when DMSO was the solvent. ^{13}C-NMR spectra were recorded on BrukerAvance™ 400 or 500 MHz spectrometers at 100 or 125 MHz. ^{19}F-NMR spectra were recorded on BrukerAvance™ 400 or 500 MHz spectrometers at 375 or 470 MHz. Multiplicities are reported using the following abbreviations: s = singlet, d = doublet, t = triplet, q = quartet, dd = doublet of doublets, ddd = doublet of doublet of doublets, td = triplet of doublets, quin = quintet, m = multiplet. Coupling constants (*J*) are given in Hertz. High-resolution electrospray ionization (HRESI) mass spectra were measured on a Waters Synapt instrument. Low-resolution electrospray ionization mass spectra (ESI-MS) were measured on a Waters 3100 mass detector. Chemical reactions were monitored by TLC (Merck, Silica gel 60 F254). Visualization was achieved using a cerium molybdate stain (5 g $(NH_4)_2Ce(NO_3)_6$, 120 g $(NH_4)_6Mo_7O_{24}\cdot 4H_2O$, 80 mL H_2SO_4, 720 mL H_2O) or with UV lamp. All chemicals, unless otherwise stated, were obtained from commercial sources. Compounds were purified using Geduran® Si 60 chromatography (Merck). The preparative reverse-phase high-pressure liquid chromatography (RP-HPLC) system used was an ECOM system equipped with a 5-µm, C-18 Phenomenex Luna Axia column (250 mm x 21.2 mm). The flow rate was 15 mL/min. Solvent A was H_2O, solvent B was acetonitrile. Analytical RP-HPLC was performed on a VWR Hitachi instrument equipped with a diode array detector and an Alltech Apollo C18 reversed-phase column (5 m, 4.6 x 250

mm). The flow rate was 1 mL/min. Solvent A was 0.1% TFA in H_2O, solvent B was acetonitrile. The SpectraMax i3x Platform spectrophotometer from Molecular Devices was used for the measurement of the excitation and absorbance spectra of the fluorescent probes.

Compound 9. 7-Diethylaminocoumarin-3-carboxylic acid[40] (61 mg, 0.23 mmol) was dissolved in dry DMF (5 mL) under argon, treated with HATU (149 mg, 0.39 mmol) and triethylamine (0.11 mL, 0.78 mmol), then stirred for 10 min at 0 °C. To the reaction mixture, **5c** (50 mg, 0.19 mmol) was added, and the solution was stirred at room temperature for 24 h. The reaction was monitored by TLC (MeOH/DCM, 1:9). Upon completion, the product was extracted with ethyl acetate, washed with H_2O, dried over $MgSO_4$, and concentrated to give the crude product. The product was isolated by column chromatography on SiO_2 using a gradient of MeOH/DCM as eluent to afford compound **9** (70 mg, 71%). HRESI-MS *m/z* calculated for $C_{26}H_{27}F_2N_4O_4$, 497.2000; found for $[M+H]^+$, 497.1996. ^{1}H NMR (400 MHz, CD_3OD) δ 8.55 – 8.51 (m, H-11, 1H), 7.53 – 7.43 (m, H-1, H-4, H-12, 3H), 6.99 – 6.91 (m, H-6, 1H), 6.90 (s, H-2, 1H), 6.84 (td, *J* = 8.4, 2.4 Hz, H-5, 1H), 6.80 – 6.73 (m, H-3, H-13, 2H), 6.51 (d, *J* = 3.2 Hz, H-14, 1H), 4.53 (d, *J* = 14.5 Hz, H-7, 1H), 4.38 (d, *J* = 14.4 Hz, H-7, 1H), 3.99 (d, *J* = 14.0 Hz, H-8, 1H), 3.89 (d, *J* = 14.0 Hz, H-8, 1H), 3.50 (q, *J* = 7.1 Hz, H-15, 4H), 1.21 (t, *J* = 7.0 Hz, H-16, 6H). ^{13}C NMR (100 MHz, CD_3OD) δ 164.84, 162.97 (dd, $^1J_{C\text{-}F}$=234.1 Hz, $^3J_{C\text{-}F}$=12.5 Hz), 162.54, 159.09 (dd, $^1J_{C\text{-}F}$=244.9 Hz, $^3J_{C\text{-}F}$=12.0 Hz), 157.78, 153.32, 148.08, 137.95, 131.29, 130.42, 126.59, 124.18, 120.70, 110.84, 110.30, 108.07, 103.52, 95.85, 75.28, 53.43, 44.58, 11.26. ^{19}F NMR (375 MHz, CD_3OD) δ -110.14 (m, F_{para}), -113.29 (m, F_{ortho}).

Compound 10. 7-Diethylaminocoumarin-3-carboxylic acid[40] (38 mg, 0.15 mmol) was dissolved in dry DMF (4 mL) under argon, treated with HATU (93 mg, 0.25 mmol) and triethylamine (0.07 mL, 0.49 mmol), then stirred for 10 min at 0 °C. To the reaction mixture, **5b**

(35 mg, 0.12 mmol) was added and the solution was stirred at room temperature for 24 h. The reaction was monitored by TLC (petroleum ether/ethyl acetate, 2:8). Upon completion, the product was extracted with ethyl acetate, washed with H_2O, dried over $MgSO_4$, and concentrated to give the crude product. The product was isolated by column chromatography on SiO_2 using a gradient of petroleum ether/ethyl acetate as eluent to afford compound **10** (65 mg, 100%). HRESI-MS *m/z* calculated for $C_{25}H_{25}Cl_2N_5O_4Na$, 552.1181; found for $[M+Na]^+$, 552.1174. ^1H NMR (500 MHz, $CDCl_3$) δ 9.17 (t, *J* = 6.0 Hz, H-9, 1H), 8.55 (s, H-10, 1H), 8.19 (s, H-2, 1H), 7.81 (s, H-1, 1H), 7.76 (d, *J* = 8.6 Hz, H-3, 1H), 7.40 – 7.33 (m, H-5, H-11, 2H), 7.15 (dd, *J* = 8.6, 2.1 Hz, H-4, 1H), 6.69 – 6.57 (m, H-8, H-12, 2H), 6.45 (d, *J* = 2.3 Hz, H-13, 1H), 4.79 (s, H-6, 2H), 4.23 (dd, *J* = 14.6, 6.3 Hz, H-7, 1H), 3.97 (dd, *J* = 14.6, 5.9 Hz, H-7, 1H), 3.44 (q, *J* = 7.1 Hz, H-14, 4H), 1.22 (t, *J* = 7.1 Hz, H-15, 6H). ^{13}C NMR (125 MHz, $CDCl_3$) δ 166.41, 162.35, 157.88, 153.02, 151.25, 148.49, 144.74, 137.08, 134.65, 131.17, 130.84, 130.57, 129.95, 129.60, 127.53, 127.28, 110.19, 108.26, 96.58, 77.93, 55.02, 47.27, 45.16, 12.40.

Compound 11. 7-Diethylaminocoumarin-3-carboxylic acid[40] (54 mg, 0.21 mmol) was dissolved in dry DMF (5 mL) under argon, treated with HATU (132 mg, 0.35 mmol) and triethylamine (0.1 mL, 0.71 mmol), then stirred for 10 min at 0 °C. To the reaction mixture, **5d** (50 mg, 0.18 mmol) was added, and the solution was stirred at room temperature for 24 h. The reaction was monitored by TLC (MeOH/DCM, 1:9). Upon completion, the product was extracted with ethyl acetate, washed with H_2O, dried over $MgSO_4$, and concentrated to give the crude product. The product was isolated by column chromatography on SiO_2 using a gradient of MeOH/DCM as eluent to afford compound **11** (88 mg, 95%). HRESI-MS *m/z* calculated for $C_{26}H_{27}Cl_2N_4O_4$, 529.1409; found for $[M+H]^+$, 529.1413. ^1H NMR (400 MHz, CD_3OD) δ 8.53 (s, H-11, 1H), 7.64 (d, *J* = 8.7 Hz, H-12, 1H), 7.52 – 7.45 (m, H-1, H-4, H-6, 3H), 7.19 (dd, *J* = 8.7,

2.2 Hz, H-5, 1H), 6.90 (s, H-2, 1H), 6.81 – 6.71 (m, H-3, H-13, 2H), 6.51 (d, *J* = 2.1 Hz, H-14, 1H), 4.91 (d, *J* = 14.5 Hz, H-7, 1H), 4.59 (s, H-9, 1H), 4.42 (d, *J* = 14.5 Hz, H-7, 1H), 4.17 (q, *J* = 14.2 Hz, H-8, 2H), 3.49 (q, *J* = 7.1 Hz, , H-15, 4H), 1.20 (t, *J* = 7.1 Hz, H-16, 6H). ^{13}C NMR (100 MHz, CD_3OD) δ 165.17, 162.72, 157.94, 153.50, 148.26, 138.03, 137.13, 134.43, 131.47, 131.08, 130.15, 129.50, 127.08, 126.63, 120.74, 110.47, 108.14, 96.01, 76.96, 52.21, 45.71, 44.74, 11.42.

Compound 12. 7-(1-Ethylpropoxy)-coumarin-3-carboxylic acid (29 mg, 0.10 mmol) was dissolved in dry DMF (1 mL) under argon, treated with HATU (74 mg, 0.19 mmol) and N,N-diisopropylethylamine (0.06 mL, 0.34 mmol), then stirred for 10 min at 0 °C. To the reaction mixture, **5a**[41] (22 mg, 0.09 mmol) was added, and the solution was stirred at room temperature for 24 h. The reaction was monitored by TLC (MeOH/DCM, 1:9). Upon completion, the product was extracted with ethyl acetate, washed with H_2O, dried over $MgSO_4$, and concentrated to give the crude product. The product was isolated by column chromatography on SiO_2 using a gradient of MeOH/DCM as eluent to afford compound **12** (33 mg, 72%). HRESI-MS *m/z* calculated for $C_{26}H_{27}F_2N_4O_5$, 513.1950; found for $[M+H]^+$, 513.1951. ^{1}H NMR (500 MHz, CD_3OD) δ 8.71 (s, H-10, 1H), 8.35 (s, H-2, 1H), 7.78 (s, H-1, 1H), 7.69 (d, *J* = 8.8 Hz, H-11, 1H), 7.51 (td, *J* = 9.0, 6.6 Hz, H-3, 1H), 7.01 – 6.91 (m, H-5, H-12, H-13, 3H), 6.85 (td, *J* = 8.4, 2.4 Hz, H-4, 1H), 4.78 (d, *J* = 14.4 Hz, H-6, 1H), 4.68 (d, *J* = 14.4 Hz, H-6, 1H), 4.41 (quin, *J* = 5.8 Hz, H-14, 1H), 4.02 (d, *J* = 13.9 Hz, H-7, 1H), 3.95 (d, *J* = 14.1 Hz, H-7, 1H), 1.78 – 1.67 (m, H-15, 4H), 0.96 (t, *J* = 7.4 Hz, H-16, 6H). ^{13}C NMR (125 MHz, CD_3OD) δ 164.81, 163.69, 163.00 (dd, $^1J_{C\text{-}F}$=246.6 Hz, $^3J_{C\text{-}F}$=12.2 Hz), 161.54, 159.43 (dd, $^1J_{C\text{-}F}$=245.6 Hz, $^3J_{C\text{-}F}$=11.9 Hz), 156.88, 150.03, 148.37, 144.75, 131.35, 130.00, 123.94, 114.69, 113.22, 111.87, 110.75, 103.65, 101.19, 80.94, 74.70, 55.59, 46.13, 25.65, 8.29. ^{19}F NMR (470 MHz, CD_3OD) δ -109.26 (m, F_{para}), -112.84 (m, F_{ortho}).

Compound 13. 7-(1-Ethylpropoxy)-coumarin-3-carboxylic acid (33 mg, 0.12 mmol) was dissolved in dry DMF (1 mL) under argon, treated with HATU (78 mg, 0.21 mmol) and N,N-diisopropylethylamine (0.07 mL, 0.40 mmol), then stirred for 10 min at 0 °C. To the reaction mixture, **5c** (29 mg, 0.11 mmol) was added, and the solution was stirred at room temperature for 24 h. The reaction was monitored by TLC (MeOH/DCM, 1:9). Upon completion, the product was extracted with ethyl acetate, washed with H_2O, dried over $MgSO_4$, and concentrated to give the crude product. The product was isolated by column chromatography on SiO_2 using a gradient of MeOH/DCM as eluent to afford compound **13** (34 mg, 60%). HRESI-MS *m/z* calculated for $C_{27}H_{28}F_2N_3O_5$, 512.1997; found for $[M+H]^+$, 512.1995. ^{1}H NMR (400 MHz, CD_3OD) δ 8.76 (s, H-11, 1H), 7.73 (d, *J* = 8.8 Hz, H-12, 1H), 7.57 – 7.47 (m, H-1, H-4, 2H), 7.05 – 6.98 (m, H-6, H-13, 2H), 6.97 (d, *J* = 2.3 Hz, H-14, 1H), 6.94 (s, H-2, 1H), 6.88 (td, *J* = 8.4, 2.4 Hz, H-5, 1H), 6.79 (s, H-3, 1H), 4.58 (d, *J* = 14.6 Hz, H-7, 1H), 4.44 (m, H-7, H-15, 2H), 4.04 (d, *J* = 14.0 Hz, H-8, 1H), 3.97 (d, *J* = 14.1 Hz, H-8, 1H), 1.82 – 1.69 (m, H-16, 4H), 1.00 (t, *J* = 7.4 Hz, H-17, 6H). ^{13}C NMR (100 MHz, CD_3OD) δ 164.82, 163.70, 163.00 (dd, $^1J_{C\text{-}F}$=246.7 Hz, $^3J_{C\text{-}F}$=12.2 Hz), 159.15 (dd, $^1J_{C\text{-}F}$=247.1 Hz, $^3J_{C\text{-}F}$=11.9 Hz), 156.87, 148.35, 137.96, 131.33, 130.48, 126.67, 120.67, 114.68, 113.27, 111.89, 110.85, 103.54, 101.22, 80.97, 75.15, 53.35, 46.36, 25.65, 8.26. ^{19}F NMR (375 MHz, CD_3OD) δ -110.11 (m, F_{para}), -113.24 (m, F_{ortho}).

Compound 14. 7-(1-Ethylpropoxy)-coumarin-3-carboxylic acid (34 mg, 0.12 mmol) was dissolved in dry DMF (1 mL) under argon, treated with HATU (83 mg, 0.22 mmol) and N,N-diisopropylethylamine (0.07 mL, 0.40 mmol), then stirred for 10 min at 0 °C. To the reaction mixture, **5b** (34 mg, 0.12 mmol) was added, and the solution was stirred at room temperature for 24 h. The reaction was monitored by TLC (MeOH/DCM, 1:9). Upon completion, the product was extracted with ethyl acetate, washed with H_2O, dried over $MgSO_4$, and concentrated to give

the crude product. The product was isolated by column chromatography on SiO_2 using a gradient of MeOH/DCM as eluent to afford compound **14** (48 mg, 73%). HRESI-MS *m/z* calculated for $C_{26}H_{27}C_{l2}N_4O_5$, 545.1359; found for [M+H]+, 545.1355. ^{1}H NMR (400 MHz, CD_3OD) δ 8.73 (s, H-10, 1H), 8.39 (s, H-2, 1H), 7.81 (s, H-1, 1H), 7.69 (t, *J* = 8.5 Hz, H-3, H-11 2H), 7.49 (d, *J* = 2.2 Hz, H-5, 1H), 7.25 (dd, *J* = 8.6, 2.2 Hz, H-4 1H), 7.00 (dd, *J* = 8.7, 2.3 Hz, H-12, 1H), 6.95 (d, *J* = 2.2 Hz, H-13, 1H), 5.12 (d, *J* = 14.4 Hz, H-6, 1H), 4.82 (d, *J* = 14.4 Hz, H-6, 1H), 4.43 (quin, *J* = 5.8 Hz, H-14, 1H), 4.28 (d, *J* = 14.2 Hz, H-7, 1H), 4.20 (d, *J* = 14.2 Hz, H-7, 1H), 1.81 – 1.69 (m, H-15, 4H), 0.99 (t, *J* = 7.4 Hz, H-16, 6H). ^{13}C NMR (125 MHz, CD_3OD) δ 164.83, 163.86, 161.55, 156.90, 150.02, 148.40, 144.83, 136.85, 134.33, 131.40, 130.83, 130.25, 126.89, 114.69, 113.12, 111.87, 101.19, 80.93, 76.17, 54.28, 45.33, 25.64, 8.28.

Compound 15. 7-(1-Ethylpropoxy)-coumarin-3-carboxylic acid (27 mg, 0.10 mmol) was dissolved in dry DMF (1.3 mL) under argon, treated with HATU (64 mg, 0.17 mmol) and N,N-diisopropylethylamine (0.06 mL, 0.34 mmol), then stirred for 10 min at 0 °C. To the reaction mixture, **5d** (25 mg, 0.09 mmol) was added, and the solution was stirred at room temperature for 24 h. The reaction was monitored by TLC (MeOH/DCM, 1:9). Upon completion, the product was extracted with ethyl acetate, washed with H_2O, dried over $MgSO_4$, and concentrated to give the crude product. The product was isolated by column chromatography on SiO_2 using a gradient of MeOH/DCM as eluent to afford compound **15** (30 mg, 63%). HRESI-MS *m/z* calculated for $C_{27}H_{28}Cl_2N_3O_5$, 544.1406; found for $[M+H]^+$, 544.1403. ^{1}H NMR (500 MHz, CD_3OD) δ 8.72 (s, H-11, 1H), 7.69 (d, *J* = 8.8 Hz, H-12, 1H), 7.65 (d, *J* = 8.7 Hz, H-4, 1H), 7.47 (m, H-1, H-6, 2H), 7.21 (dd, *J* = 8.7, 2.2 Hz, H-5, 1H), 6.99 (dd, *J* = 8.8, 2.4 Hz, H-13, 1H), 6.93 (d, *J* = 2.2 Hz, H-14, 1H), 6.91 (s, H-2, 1H), 6.75 (s, H-3, 1H), 4.93 (d, *J* = 14.5 Hz, H-7, 1H), 4.48 – 4.36 (m, H-7, H-15, 2H), 4.23 (d, *J* = 14.2 Hz, H-8, 1H), 4.18 (d, *J* = 14.2 Hz, H-8, 1H), 1.78 – 1.66 (m, H-

16, 4H), 0.96 (t, *J* = 7.4 Hz, H-17, 6H). ^{13}C NMR (125 MHz, CD_3OD) δ 164.83, 163.84, 161.58, 156.90, 148.39, 137.88, 136.86, 134.32, 131.31, 130.96, 130.14, 126.99, 126.63, 120.56, 114.69, 113.15, 111.88, 101.20, 80.94, 76.64, 51.96, 45.50, 25.64, 8.28.

Compound 16. Coumarin-3-carboxylic acid[42] (74 mg, 0.39 mmol) was dissolved in dry DMF (8 mL) under argon, treated with HATU (298 mg, 0.79 mmol) and triethylamine (0.22 mL, 1.57 mmol), then stirred for 10 min at 0 °C. To the reaction mixture, **5a**[41] (100 mg, 0.39 mmol) was added, and the solution was stirred at room temperature for 24 h. The reaction was monitored by TLC (petroleum ether/ethyl acetate, 1:9). Upon completion, the product was extracted with ethyl acetate, washed with H_2O, dried over $MgSO_4$, and concentrated to give the crude product. The product was isolated by column chromatography on SiO_2 using a gradient of petroleum ether/ethyl acetate as eluent to afford compound **16** (158 mg, 95%). HRESI-MS *m/z* calculated for $C_{21}H_{17}F_2N_4O_4$, 427.1218; found for $[M+H]^+$, 427.1213. ^{1}H NMR (500 MHz, $CDCl_3$) δ 9.16 (s, H-9, 1H), 8.82 (s, H-10, 1H), 8.10 (s, H-2, 1H), 7.84 (s, H-1, 1H), 7.72 – 7.65 (m, H-11, H-13, 2H), 7.61(m, H-3, 1H), 7.47 – 7.31 (m, H-12, H-14, 2H), 6.89 – 6.75 (m, H-4, H-5, 2H), 5.98 (s, H-8, 1H), 4.63 (q, *J* = 14.1 Hz, H-6, 2H), 3.95 (d, *J* = 6.1 Hz, H-7, 2H). ^{13}C NMR (125 MHz, $CDCl_3$) δ 164.14, 162.95 (dd, $^1J_{C\text{-}F}$=246.0 Hz, $^3J_{C\text{-}F}$=12.3 Hz), 161.03, 158.73(dd, $^1J_{C\text{-}F}$=247.4 Hz, $^3J_{C\text{-}F}$=11.5 Hz), 154.56, 151.63, 149.07, 144.58, 134.63, 130.07, 129.96, 125.48, 123.63, 118.37, 117.23, 116.76, 111.78, 104.23, 56.04, 47.81. ^{19}F NMR (470 MHz, $CDCl_3$) δ -109.52 (m, F_{para}), -109.92 (m, F_{ortho}).

Compound 17. 2-Oxo-1,2-dihydroquinoline-3-carboxylic acid (55 mg, 0.29 mmol) was dissolved in dry DMF (2 mL) under argon, treated with HATU (167 mg, 0.44 mmol) and N,N-diisopropylethylamine (0.17 mL, 0.97 mmol), then stirred for 10 min at 0 °C. To the reaction mixture, **5a**[41] (64 mg, 0.25 mmol) was added, and the solution was stirred at room temperature

for 24 h. The reaction was monitored by TLC (MeOH/DCM, 1:9). Upon completion, the product was extracted with ethyl acetate, washed with H_2O, dried over $MgSO_4$, and concentrated to give the crude product. The product was isolated by column chromatography on SiO_2 using a gradient of MeOH/DCM as eluent to afford compound **17** (43 mg, 40%). HRESI-MS *m/z* calculated for $C_{21}H_{18}F_2N_5O_3$, 426.1378; found for $[M+H]^+$, 426.1375. ^{1}H NMR (400 MHz, DMSO-d_6) δ 12.37 (s, H-15, 1H), 9.94 (t, *J* = 5.7 Hz, H-9, 1H), 8.75 (s, H-10, 1H), 8.28 (s, H-2, 1H), 7.89 (dd, *J* = 8.0, 1.0 Hz, H-11, 1H), 7.74 (s, H-1, 1H), 7.62 (ddd, *J* = 8.5, 7.3, 1.4 Hz, H-13, 1H), 7.44 – 7.34 (m, H-3, H-14, 2H), 7.28 – 7.22 (m, H-12, 1H), 7.15 (ddd, *J* = 11.9, 9.2, 2.5 Hz, H-5, 1H), 6.92 (td, *J* = 8.5, 2.5 Hz, H-4, 1H), 6.28 (s, H-8, 1H), 4.66 (d, *J* = 14.4 Hz, H-6, 1H), 4.53 (d, *J* = 14.3 Hz, H-6, 1H), 3.85 (d, *J* = 5.8 Hz, H-7, 2H). ^{13}C NMR (100 MHz, DMSO-d_6) δ 163.72, 162.34 (dd, $^1J_{C\text{-}F}$=244.5 Hz, $^3J_{C\text{-}F}$=12.7 Hz), 162.26, 159.51 (dd, $^1J_{C\text{-}F}$=245.9 Hz, $^3J_{C\text{-}F}$=12.1 Hz), 151.07, 145.41, 144.46, 139.86, 133.23, 130.72, 130.22, 125.12, 123.27, 121.59, 118.96, 115.70, 111.30, 104.42, 74.77, 55.70, 46.26. ^{19}F NMR (375 MHz, DMSO-d_6) δ -107.97 (m, F_{para}), -112.31 (m, F_{ortho}).

Compound 18. 7-Methoxy-coumarin-3-carboxylic acid[43] (54 mg, 0.25 mmol) was dissolved in dry DMF (3 mL) under argon, treated with HATU (166 mg, 0.44 mmol) and N,N-diisopropylethylamine (0.14 mL, 0.80 mmol), then stirred for 10 min at 0 °C. To the reaction mixture, **5a**[41] (53 mg, 0.21 mmol) was added, and the solution was stirred at room temperature for 24 h. The reaction was monitored by TLC (MeOH/DCM, 1:9). Upon completion, the product was extracted with ethyl acetate, washed with H_2O, dried over $MgSO_4$, and concentrated to give the crude product. The product was isolated by column chromatography on SiO_2 using a gradient of MeOH/DCM as eluent to afford compound **18** (78 mg, 82%). HRESI-MS *m/z* calculated for $C_{22}H_{19}F_2N_4O_5$, 457.1324; found for $[M+H]^+$, 457.1317. ^{1}H NMR (400 MHz, DMSO-d_6) δ 8.88 –

8.80 (m, H-9, H-10, 2H), 8.32 (s, H-2, 1H), 7.91 (d, *J* = 8.8 Hz, H-11, 1H), 7.78 (s, H-1, 1H), 7.43 (dd, *J* = 15.9, 8.9 Hz, H-3, 1H), 7.19 (ddd, *J* = 11.8, 9.2, 2.4 Hz, H-5, 1H), 7.11 (d, *J* = 2.2 Hz, H-13, 1H), 7.05 (dd, *J* = 8.7, 2.3 Hz, H-12, 1H), 6.98 (td, *J* = 8.6, 2.4 Hz, H-4, 1H), 6.35 (s, H-8, 1H), 4.68 (d, *J* = 14.4 Hz, H-6, 1H), 4.58 (d, *J* = 14.4 Hz, H-6, 1H), 3.95 – 3.79 (m, H-7, H-14, 5H). ^{13}C NMR (125 MHz, $CDCl_3$) δ 165.35, 164.88, 162.89 (dd, $^{1}J_{C\text{-}F}$=250.0 Hz, $^{3}J_{C\text{-}F}$=12.0 Hz), 161.43, 158.73 (dd, $^{1}J_{C\text{-}F}$=246.3 Hz, $^{3}J_{C\text{-}F}$=11.8 Hz), 156.90, 151.52, 148.95, 144.59, 131.13, 130.36, 123.74, 114.32, 113.35, 112.16, 111.71, 104.19, 100.35, 56.11, 47.85. ^{19}F NMR (470 MHz, $CDCl_3$) δ -109.49 (m, F_{para}), -110.11 (m, F_{ortho}).

Compound 19. 7-Methoxy-2-oxo-1,2-dihydroquinoline-3-carboxylic acid (38 mg, 0.17 mmol) was dissolved in dry DMF (2 mL) under argon, treated with HATU (146 mg, 0.39 mmol) and N,N-diisopropylethylamine (0.12 mL, 0.69 mmol), then stirred for 10 min at 0 °C. To the reaction mixture, **5a**[41] (46 mg, 0.18 mmol) was added, and the solution was stirred at room temperature for 24 h. The reaction was monitored by TLC (MeOH/DCM, 1:9). Upon completion, the product was extracted with ethyl acetate, washed with H_2O, dried over $MgSO_4$, and concentrated to give the crude product. The product was isolated by column chromatography on SiO_2 using a gradient of MeOH/DCM as eluent to afford compound **19** (24 mg, 30%). HRESI-MS *m/z* calculated for $C_{22}H_{20}F_2N_5O_4$, 456.1483; found for $[M+H]^+$, 456.1480. ^{1}H NMR (400 MHz, DMSO-d_6) δ 9.98 (t, *J* = 5.3 Hz, H-9, 1H), 8.67 (s, H-10, 1H), 8.33 (s, H-2, 1H), 7.80 (d, *J* = 8.7 Hz, H-11, 1H), 7.75 (s, H-1, 1H), 7.42 (dd, *J* = 15.9, 8.9 Hz, H-3, 1H), 7.16 (ddd, *J* = 11.7, 9.2, 2.4 Hz, H-5, 1H), 7.00 – 6.82 (m, H-4, H-12, H-13, 3H), 6.46 (s, H-8, 1H), 4.68 (d, *J* = 14.3 Hz, H-6, 1H), 4.56 (d, *J* = 14.3 Hz, H-6, 1H), 3.94 – 3.76 (m, H-7, H-15, 5H). ^{13}C NMR (100 MHz, DMSO-d_6) δ 164.33, 163.37, 162.84, 162.30 (dd, $^{1}J_{C\text{-}F}$=244.2 Hz, $^{3}J_{C\text{-}F}$=12.4 Hz), 159.50 (dd, $^{1}J_{C\text{-}F}$=246.0 Hz, $^{3}J_{C\text{-}F}$=12.2 Hz), 151.04, 145.43, 143.99, 142.49, 131.80, 130.75,

125.24, 118.20, 113.47, 112.92, 111.26, 104.37, 98.11, 74.84, 56.06, 55.87, 46.30. ^{19}F NMR (375 MHz, DMSO-d_6) δ -107.98 (m, F_{para}), -112.34 (m, F_{ortho}).

Compound 20. 7-Chloro-2-oxo-1,2-dihydroquinoline-3-carboxylic acid (55 mg, 0.25 mmol) was dissolved in dry DMF (3 mL) under argon, treated with HATU (192 mg, 0.51 mmol) and N,N-diisopropylethylamine (0.17 mL, 0.97 mmol), then stirred for 10 min at 0 °C. To the reaction mixture, **5a**[41] (56 mg, 0.22 mmol) was added, and the solution was stirred at room temperature for 24 h. The reaction was monitored by TLC (MeOH/DCM, 1:9). Upon completion, the product was extracted with ethyl acetate, washed with H_2O, dried over $MgSO_4$, and concentrated to give the crude product. The product was isolated by column chromatography on SiO_2 using a gradient of MeOH/DCM as eluent to afford compound **20** (60 mg, 59%). HRESI-MS *m/z* calculated for $C_{21}H_{17}F_2N_5O_3$, 460.0988; found for $[M+H]^+$, 460.0982. ^{1}H NMR (400 MHz, DMSO-d_6) δ 12.49 (s, H-14, 1H), 9.94 (s, H-9, 1H), 8.79 (s, H-10, 1H), 8.33 (s, H-2, 1H), 7.97 (d, *J* = 8.6 Hz, H-11, 1H), 7.78 (s, H-1, 1H), 7.47 – 7.38 (m, H-3, H-13, 2H), 7.32 (dd, *J* = 8.5, 2.0 Hz, H-12, 1H), 7.19 (ddd, *J* = 11.8, 9.2, 2.5 Hz, H-5, 1H), 6.96 (td, *J* = 8.5, 2.4 Hz, H-4, 1H), 6.34 (s, H-8, 1H), 4.69 (d, *J* = 14.4 Hz, H-6, 1H), 4.57 (d, *J* = 14.3 Hz, H-6, 1H), 3.89 (d, *J* = 5.7 Hz, H-7, 2H). ^{13}C NMR (100 MHz, DMSO-d_6) δ 163.58, 162.45, 162.30 (dd, $^1J_{C-F}$=231.0 Hz, $^3J_{C-F}$=13.1 Hz), 159.50 (dd, $^1J_{C-F}$=246.3 Hz, $^3J_{C-F}$=12.0 Hz), 151.08, 145.41, 143.76, 141.03, 137.52, 132.07, 130.71, 125.17, 123.39, 121.81, 117.88, 115.25, 111.30, 104.41, 74.76, 55.69, 46.26. ^{19}F NMR (375 MHz, DMSO-d_6) δ -107.97 (m, F_{para}), -112.29 (m, F_{ortho}).

Compound 21. 7-Hydroxycoumarin-3-carboxylic acid[43] (40 mg, 0.19 mmol) was dissolved in dry DMF (6 mL) under argon, treated with HATU (148 mg, 0.39 mmol) and triethylamine (0.11 mL, 0.78 mmol), then stirred for 10 min at 0 °C. To the reaction mixture, **5a**[41] (50 mg, 0.19 mmol) was added, and the solution was stirred at room temperature for 24 h. The reaction was

monitored by TLC (MeOH/DCM, 1:9). Upon completion, the product was extracted with ethyl acetate, washed with H_2O, dried over $MgSO_4$, and concentrated to give the crude product. The product was isolated by column chromatography on SiO_2 using a gradient of MeOH/DCM as eluent to afford compound **21** (70 mg, 81%). HRESI-MS *m/z* calculated for $C_{21}H_{16}F_2N_4O_5Na$, 465.0986; found for $[M+Na]^+$, 465.0978. ^{1}H NMR (400 MHz, CD_3OD) δ 8.69 (s, H-10, 1H), 8.34 (s, H-2, 1H), 7.77 (s, H-1, 1H), 7.62 (d, *J* = 8.7 Hz, H-11, 1H), 7.50 (td, *J* = 9.0, 6.6 Hz, H-3, 1H), 6.94 (ddd, *J* = 11.7, 8.8, 2.5 Hz, H-5, 1H), 6.88 – 6.80 (m, H-4, H-12, 2H), 6.73 (d, *J* = 1.9 Hz, H-13, 1H), 4.75 (m, H-6, 1H), 4.66 (d, *J* = 14.3 Hz, H-6, 1H), 4.53 (s, H-8, 1H), 4.01 (d, *J* = 14.1 Hz, H-7, 1H), 3.94 (d, *J* = 14.3 Hz, H-7, 1H). ^{13}C NMR (125 MHz, DMSO-d_6) δ 164.94, 162.54, 162.35 (dd, $^1J_{C\text{-}F}$=246.5 Hz, $^3J_{C\text{-}F}$=13.0 Hz), 161.57, 159.51 (dd, $^1J_{C\text{-}F}$=246.3 Hz, $^3J_{C\text{-}F}$=12.1 Hz), 156.89, 151.12, 148.79, 145.44, 132.54, 130.66, 125.08, 115.18, 112.14, 111.43, 111.27, 104.48, 102.27, 74.67, 55.60, 46.15. ^{19}F NMR (375 MHz, CD_3OD) δ -109.70 (m, F_{para}), -113.29 (m, F_{ortho}).

Biological assays

Preparation of stock solutions of the tested compounds: Compounds **8**-**21** were dissolved in anhydrous DMSO to final concentrations of 5 mg/mL. The antifungal drugs **1**-**7** were purchased from Sigma Aldrich. All antifungal agents were dissolved in anhydrous DMSO to a final concentration of 5 mg/mL.

Minimal inhibitory concentration broth double-dilution assay: Minimal inhibitory concentrations (MICs) were determined using the double-dilution method in 96-well plates

(Corning). Yeast strains were grown in Casitone broth that was prepared from 9 g Casitone (bacto-casitone), 5 g yeast extract, 11.5 g sodium citrate dihydrate, 20 g glucose to a final volume of 1000 mL. Starter cultures were incubated for 24 h or 48 h (37 °C, 5% CO_2, aerobic conditions) and then diluted 1:100 into fresh medium. Compounds dissolved in DMSO were added to Casitone (32 µL stock solution in 1218 µL of Casitone), and serial double dilutions of compounds in Casitone were prepared in flat-bottomed 96-well microplates (Corning) to enable testing of concentrations ranging from 64 µg/mL to 0.007 µg/mL. Control wells with no compounds and wells without yeast cells containing each tested concentration of the compounds (blanks) were also prepared. An equal volume (100 µL) of yeast suspensions in Casitone broth was added to each well. The DMSO concentrations ranged from 0.0012% to 1.3%. The final inoculum was between 5 x 10^4 CFU/mL and 5 x 10^5 CFU/mL. After incubation for 24 h at 37 °C in 5% CO_2, MTT (50 µL of a 1 mg/mL solution in ddH_2O) was added to each well followed by additional incubation at 37 °C for 2 h. MIC values were defined as the lowest concentration of an antifungal agent that causes a specified reduction in visible growth as per the CLSI M27-A3 protocol. The magnitude of reduction in visible growth was assessed using the following numerical scale: 0, optically clear; 1, slightly hazy; 2, prominent decrease (~50%) in visible growth; 3, slightly reduction in visible growth; and 4, no reduction in visible growth. The MIC was defined based on reduction in growth to 0 or 1. Results were confirmed in two independent experiments, and each concentration was tested in triplicate.

Live cell imaging: Cells were grown to log phase in liquid yeast extract peptone dextrose overnight at 30 °C in a 10 mL tube. Cells were diluted 1:10 and then incubated for 2 h at 30 °C to log phase. The azoles **8** and **9** were added to a final concentration of 10 µM. Cells were then

incubated in the dark for a total of 60 min. Before imaging, cells were washed once with PBS buffer. A 2-μL aliquot of *Candida* cell sample was placed on a glass slide and covered with a glass coverslip. The cells were imaged on a MORE imaging system (TILL Photonics GmbH) with an Olympus UPlanApo 100X 1.3 NA oil immersion objective. The bandpass filter sets used to image compound **8** and **9** were excitation 427/10 nm and emission 510/20 nm.

Disk-diffusion assay: Antifungal activity against *C. albicans* SN152 and against *C. albicans erg11*ΔΔ *erg3*ΔΔ was confirmed by the disk diffusion assay. Strains were streaked from frozen culture onto a YPD agar plate that was prepared from 65 g of YPD agar (Sigma) in a final volume of 1000 mL. Plates were incubated for 24 h at 30 °C for *C. albicans* SN152 and 48 h for *C. albicans erg11*ΔΔ *erg3*ΔΔ. Two or three colonies were placed into 1 mL of PBS solution, and optical density (OD) was determined with a TECAN Infinite. OD was adjusted to 0.02 for *C. albicans* SN152 and to 0.03 for *C. albicans erg11*ΔΔ *erg3*ΔΔ by dilution with PBS, and 200 μL of diluted culture from each strain was plated onto 15-mL Casitone plates and spread using sterile beads (3 mm, Fisher Scientific). After the plates dried, a single disk (6-mm diameter, Becton Dickinson) with 25 μg of the drug being tested was placed in the center of each plate. Plates were then incubated at 30 °C and photographed under the same imaging conditions after 24 h.

CYP3A4 inhibition assay: CYP3A4 activity was determined using a P450-Glo CYP3A4 assay kit with Luciferin-PPXE according to manufacturer's protocol. Briefly, CYP3A4 reactions were carried out in a white polystyrene 96-well flat-bottom plate (Corning) by mixing 12.5 μL of test compounds with 12.5 μL of membrane preparations containing recombinant human CYP3A4.

Controls were 12.5 µL of vehicle mixed with 12.5 µL of membranes without CYP3A4. The plate was pre-incubated at 37 °C for 10 min, and then 25 µL of NADPH regeneration reagent was added to initiate the CYP3A4 reaction. The assay mixture was mixed briefly, and the plate was incubated at 37 °C. After 15 min, 50 µL of reconstituted Luciferin Detection Reagent (Promega) was then added to all the wells to terminate the CYP3A4 reaction. The reaction mixture was mixed briefly and the plate was incubated at room temperature for 20 min to stabilize the luminescent signal. Luminescence was measured using a TECAN microplate reader (Infinite F200 Pro).

Cell viability assay: HEK-293T cells were cultured in DMEM medium (Thermo Fisher Scientific) supplemented with 10% fetal bovine serum (Thermo Fisher Scientific), 1% MEM NEAA (Thermo Fisher Scientific), 1% sodium pyruvate (Thermo Fisher Scientific) and 1% Penicillin-Streptomycin-Nystatin (Biological Industries). HepG2 cells were cultured in RPMI medium (Thermo Fisher Scientific) supplemented with 15% fetal bovine serum, 1% MEM NEAA, 1% sodium pyruvate, and 1% penicillin-streptomycin-nystatin. Cells were kept at a temperature of 37 °C, with 5% CO_2 and 100% humidity. For analyses, 4000 HepG2 or 7000 HEK-293T cells in 70 µL were seeded in wells of 384-well microplates (Greiner) pre-coated with poly-D-lysine (10 µg/mL, Millipore). After 24 hours, medium was replaced to 50 µL/well of fresh medium, and compounds were added at concentrations ranging from 5 to 50 µM using a D300e Digital Dispenser (Tecan) from 1 mM stocks in 10% DMSO, 0.3% Tween in PBS. After an additional 24 hours, 25 µL of XTT reagent solution (Biological Industries) was added to each well. Plates were incubated for 2 hours at 37 °C, and the absorbance of the wells was measured at 475 nm with reference at 660 nm using a Magellan M1000 pro plate reader (Tecan).

Automated cell seeding, media replacement, and XTT addition was performed using EVO 200 Liquid Handling Robotic System (Tecan).

Supplementary Material

Atom numbering systems; synthetic schemes for the preparation of intermediate compounds; detailed procedures for the preparation of intermediate compounds, absorption and emission spectra; analytical HPLC data; yeast strains; ^{1}H, ^{19}F, and ^{13}C NMR of compounds **9-21**.

Funding Sources

This work was supported by Israel Science Foundation Grant 6/14 (Micha Fridman).

Notes

The authors declare no competing financial interests.

ACKNOWLEDGMENT

We thank Y. Ebenstein for granting us access to his fluorescent microscope systems. We thank J. Berman for providing *Candida* strains.

REFERENCES

[1] R.S. Shapiro, N. Robbins, L.E. Cowen, Regulatory Circuitry Governing Fungal Development, Drug Resistance, and Disease, Microbiol. Mol. Biol. Rev. 75 (2011) 213–267. doi:10.1128/mmbr.00045-10.

[2] G.D. Brown, D.W. Denning, N.A.R. Gow, S.M. Levitz, M.G. Netea, T.C. White, Hidden killers: Human fungal infections, Sci. Transl. Med. 4 (2012). doi:10.1126/scitranslmed.3004404.

[3] L.E. Cowen, W.J. Steinbach, Stress, Drugs, and Evolution: the Role of Cellular Signaling in Fungal Drug Resistance, Eukaryot. Cell. 7 (2008) 747–764. doi:10.1128/ec.00041-08.

[4] J.B. Anderson, Evolution of antifungal-drug resistance: Mechanisms and pathogen fitness, Nat. Rev. Microbiol. 3 (2005) 547–556. doi:10.1038/nrmicro1179.

[5] A. Lupetti, R. Danesi, M. Campa, M. Del Tacca, S. Kelly, Molecular basis of resistance to azole antifungals, Trends Mol. Med. 8 (2002) 76–81. doi:10.1016/S1471-4914(02)02280-3.

[6] N. Thamban Chandrika, S.K. Shrestha, H.X. Ngo, O. V. Tsodikov, K.C. Howard, S. Garneau-Tsodikova, Alkylated Piperazines and Piperazine-Azole Hybrids as Antifungal Agents, J. Med. Chem. 61 (2018) 158–173. doi:10.1021/acs.jmedchem.7b01138.

[7] A.H. Fairlamb, N.A.R. Gow, K.R. Matthews, A.P. Waters, Drug resistance in eukaryotic microorganisms, Nat. Microbiol. 1 (2016) 16092. doi:10.1038/nmicrobiol.2016.92.

[8] M.A. Ghannoum, L.B. Rice, Antifungal agents: Mode of action, mechanisms of resistance, and correlation of these mechanisms with bacterial resistance, Clin. Microbiol. Rev. 12 (1999) 501–517. doi:10.1128/CMR.12.4.501.

[9] F.C. Odds, A.J.P. Brown, N.A.R. Gow, Antifungal agents: mechanisms of action, Trends Microbiol. 11 (2003) 272–279. doi:10.1016/S0966-842X(03)00117-3.

[10] D.J. Krysan, The unmet clinical need of novel antifungal drugs, Virulence. 8 (2017) 135–137. doi:10.1080/21505594.2016.1276692.

[11] J.A. Como, W.E. Dismukes, Oral Azole Drugs as Systemic Antifungal Therapy, N. Engl. J. Med. 330 (1994) 263–272. doi:10.1056/NEJM199401273300407.

[12] M. Kneale, J.S. Bartholomew, E. Davies, D.W. Denning, Global access to antifungal therapy and its variable cost, J. Antimicrob. Chemother. 71 (2016) 3599–3606.

doi:10.1093/jac/dkw325.

[13] W.D. Nes, Biosynthesis of Cholesterol and Other Sterols, Chem. Rev. 111 (2011) 6423–6451. doi:10.1021/cr200021m.

[14] G.I. Lepesheva, M.R. Waterman, Sterol 14α-demethylase cytochrome P450 (CYP51), a P450 in all biological kingdoms, Biochim. Biophys. Acta - Gen. Subj. 1770 (2007) 467–477. doi:10.1016/j.bbagen.2006.07.018.

[15] L. Friggeri, T.Y. Hargrove, Z. Wawrzak, A.L. Blobaum, G. Rachakonda, C.W. Lindsley, F. Villalta, W.D. Nes, M. Botta, F.P. Guengerich, G.I. Lepesheva, Sterol 14α-Demethylase Structure-Based Design of VNI ((R)- N-(1-(2,4-Dichlorophenyl)-2-(1 H-imidazol-1-yl)ethyl)-4-(5-phenyl-1,3,4-oxadiazol-2-yl)benzamide)) Derivatives to Target Fungal Infections: Synthesis, Biological Evaluation, and Crystallographic A, J. Med. Chem. 61 (2018) 5679–5691. doi:10.1021/acs.jmedchem.8b00641.

[16] S. Doß, H. Potschka, F. Doß, S. Mitzner, M. Sauer, Hepatotoxicity of antimycotics used for invasive fungal infections: In vitro results, Biomed Res. Int. 2017 (2017). doi:10.1155/2017/9658018.

[17] T. Sakaeda, K. Iwaki, M. Kakumoto, M. Nishikawa, T. Niwa, J. Jin, T. Nakamura, K. Nishiguchi, N. Okamura, K. Okumura, Effect of micafungin on cytochrome P450 3A4 and multidrug resistance protein 1 activities, and its comparison with azole antifungal drugs, J. Pharm. Pharmacol. 57 (2005) 759–764. doi:10.1211/0022357056118.

[18] M.P. Godamudunage, A.M. Grech, E.E. Scott, Comparison of antifungal azole interactions with adult cytochrome P450 3A4 versus neonatal cytochrome P450 3A7, Drug Metab. Dispos. 46 (2018) 1329–1337. doi:10.1124/dmd.118.082032.

[19] T.Y. Hargrove, L. Friggeri, Z. Wawrzak, A. Qi, W.J. Hoekstra, R.J. Schotzinger, J.D.

York, F. Peter Guengerich, G.I. Lepesheva, Structural analyses of Candida albicans sterol 14α-demethylase complexed with azole drugs address the molecular basis of azole-mediated inhibition of fungal sterol biosynthesis, J. Biol. Chem. 292 (2017) 6728–6743. doi:10.1074/jbc.M117.778308.

[20] H. Fakhim, S. Emami, A. Vaezi, S.M. Hashemi, L. Faeli, K. Diba, E. Dannaoui, H. Badali, In Vitro Activities of Novel Azole Compounds ATTAF-1 and ATTAF-2 against Fluconazole-Susceptible and -Resistant Isolates of Candida Species, Antimicrob. Agents Chemother. 61 (2017) e01106-16. doi:10.1128/aac.01106-16.

[21] A.G.S. Warrilow, C.M. Hull, J.E. Parker, E.P. Garvey, W.J. Hoekstra, W.R. Moore, R.J. Schotzinger, D.E. Kelly, S.L. Kelly, The Clinical Candidate VT-1161 Is a Highly Potent Inhibitor of Candida albicans CYP51 but Fails To Bind the Human Enzyme, Antimicrob. Agents Chemother. 58 (2014) 7121–7127. doi:10.1128/aac.03707-14.

[22] K. Motahari, H. Badali, S.M. Hashemi, H. Fakhim, H. Mirzaei, A. Vaezi, M. Shokrzadeh, S. Emami, Discovery of benzylthio analogs of fluconazole as potent antifungal agents, Future Med. Chem. 10 (2018) 987–1002. doi:10.4155/fmc-2017-0295.

[23] C. Sheng, W. Zhang, H. Ji, M. Zhang, Y. Song, H. Xu, J. Zhu, Z. Miao, Q. Jiang, J. Yao, Y. Zhou, J. Zhu, J. Lü, Structure-based optimization of azole antifungal agents by CoMFA, CoMSIA, and molecular docking, J. Med. Chem. 49 (2006) 2512–2525. doi:10.1021/jm051211n.

[24] N. Thamban Chandrika, S.K. Shrestha, H.X. Ngo, O. V. Tsodikov, K.C. Howard, S. Garneau-Tsodikova, Alkylated Piperazines and Piperazine-Azole Hybrids as Antifungal Agents, J. Med. Chem. 61 (2018) 158–173. doi:10.1021/acs.jmedchem.7b01138.

[25] J.M. Hutzler, R.J. Melton, J.M. Rumsey, M.E. Schnute, C.W. Locuson, L.C. Wienkers,

Inhibition of cytochrome P450 3A4 by a pyrimidineimidazole: Evidence for complex heme interactions, Chem. Res. Toxicol. 19 (2006) 1650–1659. doi:10.1021/tx060198m.

[26] U.M. Zanger, M. Schwab, Cytochrome P450 enzymes in drug metabolism: Regulation of gene expression, enzyme activities, and impact of genetic variation, Pharmacol. Ther. 138 (2013) 103–141. doi:10.1016/j.pharmthera.2012.12.007.

[27] T. Niwa, T. Shiraga, A. Takagi, Effect of Antifungal Drugs on Cytochrome P450 (CYP) 2C9, CYP2C19, and CYP3A4 Activities in Human Liver Microsomes, Biol. Pharm. Bull. 28 (2005) 1805–1808. doi:10.1248/bpb.28.1805.

[28] M. Shakoury-Elizeh, O. Protchenko, A. Berger, J. Cox, K. Gable, T.M. Dunn, W.A. Prinz, M. Bard, C.C. Philpott, Metabolic Response to Iron Deficiency in Saccharomyces cerevisiae, J. Biol. Chem. 285 (2010) 14823–14833. doi:10.1074/jbc.M109.091710.

[29] R.I. Benhamou, M. Bibi, K.B. Steinbuch, H. Engel, M. Levin, Y. Roichman, J. Berman, M. Fridman, Real-Time Imaging of the Azole Class of Antifungal Drugs in Live Candida Cells, ACS Chem. Biol. 12 (2017) 1769–1777. doi:10.1021/acschembio.7b00339.

[30] R.I. Benhamou, M. Bibi, J. Berman, M. Fridman, Localizing Antifungal Drugs to the Correct Organelle Can Markedly Enhance their Efficacy, Angew. Chemie - Int. Ed. 57 (2018) 6230–6235. doi:10.1002/anie.201802509.

[31] S. Brunke, B. Hube, Two unlike cousins: Candida albicans and C.glabrata infection strategies, Cell. Microbiol. 15 (2013) 701–708. doi:10.1111/cmi.12091.

[32] A.A. Sagatova, M. V. Keniya, R.K. Wilson, M. Sabherwal, J.D.A. Tyndall, B.C. Monk, Triazole resistance mediated by mutations of a conserved active site tyrosine in fungal lanosterol 14α-demethylase, Sci. Rep. 6 (2016) 26213. doi:10.1038/srep26213.

[33] T.Y. Hargrove, L. Friggeri, Z. Wawrzak, A. Qi, W.J. Hoekstra, R.J. Schotzinger, J.D.

York, F. Peter Guengerich, G.I. Lepesheva, Structural analyses of Candida albicans sterol 14α-demethylase complexed with azole drugs address the molecular basis of azole-mediated inhibition of fungal sterol biosynthesis, J. Biol. Chem. 292 (2017) 6728–6743. doi:10.1074/jbc.M117.778308.

[34] B.M. Vincent, A.K. Lancaster, R. Scherz-Shouval, L. Whitesell, S. Lindquist, Fitness Trade-offs Restrict the Evolution of Resistance to Amphotericin B, PLoS Biol. 11 (2013) e1001692. doi:10.1371/journal.pbio.1001692.

[35] C.M. Martel, J.E. Parker, O. Bader, M. Weig, U. Gross, A.G.S. Warrilow, D.E. Kelly, S.L. Kelly, A Clinical Isolate of Candida albicans with Mutations in ERG11 and ERG5 is Cross Resistant to Azoles and Amphotericin B, Antimicrob. Agents Chemother. 54 (2010) 3578–3583. doi:10.1128/AAC.00303-10.

[36] A. Rosenberg, I. V. Ene, M. Bibi, S. Zakin, E.S. Segal, N. Ziv, A.M. Dahan, A.L. Colombo, R.J. Bennett, J. Berman, Antifungal tolerance is a subpopulation effect distinct from resistance and is associated with persistent candidemia, Nat. Commun. 9 (2018) 2470. doi:10.1038/s41467-018-04926-x.

[37] D. Kim, Y. Liu, R.I. Benhamou, H. Sanchez, A. Simon-Soro, Y. Li, G. Hwang, M. Fridman, D.R. Andes, H. Koo, Bacterial-derived exopolysaccharides enhance antifungal drug tolerance in a cross-kingdom oral biofilm, ISME J. 12 (2018) 1427–1442. doi:10.1038/s41396-018-0113-1.

[38] S. Ramasamy, L.V. Kiew, L.Y. Chung, Inhibition of human cytochrome P450 enzymes by Bacopa monnieri standardized extract and constituents, Molecules. 19 (2014) 2588–2601. doi:10.3390/molecules19022588.

[39] R.I. Benhamou, Q.Z. Jaber, I.M. Herzog, Y. Roichman, M. Fridman, Fluorescent Tracking

of the Endoplasmic Reticulum in Live Pathogenic Fungal Cells, ACS Chem. Biol. 13 (2018) 3325–3332. doi:10.1021/acschembio.8b00782.

[40] K. Huang, L. Yu, P. Xu, X. Zhang, W. Zeng, A novel FRET-based ratiometric fluorescent probe for highly sensitive detection of hydrogen sulfide, RSC Adv. 5 (2015) 17797–17801. doi:10.1039/c4ra16578k.

[41] V.S. Pore, S.G. Agalave, P. Singh, P.K. Shukla, V. Kumar, M.I. Siddiqi, Organic & Biomolecular Chemistry Design and synthesis of new fluconazole analogues, Org. Biomol. Chem. 13 (2015) 6551–6561. doi:10.1039/c5ob00590f.

[42] Z. Zhang, Z.W. Bai, Y. Ling, L.Q. He, P. Huang, H.X. Gu, R.F. Hu, Design, synthesis and biological evaluation of novel furoxan-based coumarin derivatives as antitumor agents, Med. Chem. Res. 27 (2018) 1198–1205. doi:10.1007/s00044-018-2140-x.

[43] C.Y. Ng, T.X.W. Kwok, F.C.K. Tan, C.-M. Low, Y. Lam, Fluorogenic probes to monitor cytosolic phospholipase A 2 activity, Chem. Commun. 53 (2017) 1813–1816. doi:10.1039/C6CC09305A.

The highlighted findings of this study are:

1. Imidazole-based aminocoumarin antifungals had superior potency compared to triazoles.
2. Imidazole antifungals reduced trailing growth associated with reoccurring infections.
3. Triazoles targeted CYP51, whereas imidazoles had additional modes of action.
4. Triazoles were less toxic to mammalian cells than imidazoles.
5. Aminocoumarin antifungals localized to the endoplasmic reticulum in *Candida* cells.